

## Radar echo characteristics at Ny-Ålesund, Svalbard and Arctic storms over the Norwegian Sea

Yoshio Asuma<sup>1\*</sup>, Nao Ogitani<sup>1</sup> and Makoto Wada<sup>2</sup>

<sup>1</sup>*Division of Earth and Planetary Sciences, Graduate School of Science, Hokkaido University, Kita-10, Nishi-8, Kita-ku, Sapporo 060-0810*

<sup>2</sup>*National Institute of Polar Research, Kaga 1-chome, Itabashi-ku, Tokyo 173-8515*

\*Corresponding author. E-mail: [asuma@ep.sci.hokudai.ac.jp](mailto:asuma@ep.sci.hokudai.ac.jp)

(Received March 1, 2005; Accepted August 24, 2005)

**Abstract:** This paper is a preliminary report on radar echo characteristics and Arctic storms near Svalbard. Using an X-band vertically pointing radar data at Ny-Ålesund, Svalbard, Norway and synoptic weather charts, the radar echo characteristics are investigated for one year between April 1994 and March 1995. Radar echoes have distinct seasonal variations with respect to height. Taking account of synoptic conditions, each series of radar echoes is classified into four patterns and it is found that they have strong seasonal variations. The low pressure system echo patterns appear throughout the year; their appearance frequencies exceed 50% of all radar echo appearances and increase in early summer and early winter. The appearance frequencies of low pressure systems over the Norwegian Sea have also characteristic strong seasonal variations. These low pressure activities appear to be related to precipitation behavior at Ny-Ålesund and vapor transportation to the high Arctic from lower latitudes.

**key words:** radar echo, climatology, Arctic storms, Ny-Ålesund

### 1. Introduction

Arctic synoptic scale climatology has been described by Serreze and Barry (1988, 1995), Serreze *et al.* (1993) and Cullather *et al.* (2000). Serreze and Barry (1995) reports climatological characteristics of the vapor behavior at 70°N. They suggest that a large amount of annual poleward vapor transportation is found over the Norwegian Sea and Baffin Bay. Indeed, the Norwegian Sea region is unique from the viewpoint of global energy and water circulation. Even in mid-winter, the open sea surface extends into the polar cap due to the warm Gulf Stream. Considerable water and heat are supplied to the atmosphere from the open sea surface. Severe Arctic disturbances frequently appear and travel over the Norwegian Sea. They bring a large amount of water vapor into the Arctic region, which precipitates out and may feed glaciers and ice sheets (cryosphere). This vapor flow can be identified by satellite microwave observation. Newell and Zhu (1994) called this vapor stream a “Tropospheric river.” They also pointed out a possibility to apply this concept to ice core analyses. The interaction

with climate is one of the main topics of the CliC (Climate and cryosphere) project (Allison *et al.*, 2001). Recently, Oshima and Yamazaki (2004) have reported on the climatological seasonal variations of the moisture transport and its budget ( $P-E$ ; Precipitation minus evaporation/sublimation) in the Arctic and Antarctic regions and discuss the annual modes (AO; Arctic Oscillation and AAO; Antarctic Oscillation).

In spite of the importance of precipitation in the polar region, direct investigations of Arctic storms are sparse, especially direct measurements of precipitation by weather radar. To better understand the distribution and behavior of water in the polar region, it is necessary to monitor precipitation by weather radar. But at present only a few radar systems are collecting data in the Arctic and Antarctic regions. The National Institute of Polar Research (NIPR) set up a vertically pointing weather radar system at Ny-Ålesund, Svalbard, Norway and successfully collected data from April 1994 to March 1995. In this paper, using this data set, we present a preliminary report on statistical properties of radar echoes.

## 2. Analyzed data set

Figure 1 shows the location of Ny-Ålesund ( $78^{\circ}55'N$ ,  $11^{\circ}56'E$ ), Norway. Ny-Ålesund is located in a fjord on the northwestern coast of the Svalbard archipelago. NIPR set up an X-band vertically pointing radar (Wave length:  $\lambda=3.2$  cm, Antenna diameter:  $\phi=2.4$  m, Peak power:  $W_p=40$  kW) at Ny-Ålesund in 1992 (Wada *et al.*, 1997). The radar system measured radar reflectivity every 10 s up to 6.4 km AGL

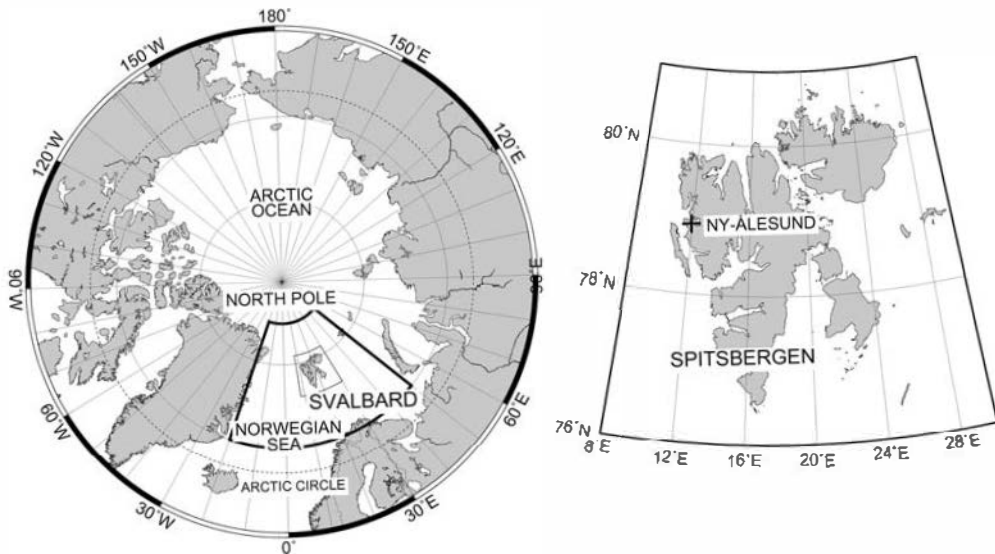


Fig. 1. Maps of the experimental region. The Spitsbergen region is shown in the thin sector in the left panel. The right panel shows an enlarged map of the Svalbard archipelago. The location of Ny-Ålesund is shown as a thick cross mark in the right panel. The thick sector in the left panel shows the analyzed area in Section 4.

(above ground level) with 50 m resolution. Radar reflectivity stronger than 0 dBZ was averaged at 30 min intervals and used for analysis. NIPR intermittently operated the radar system starting in August 1992, and continuously collected radar data throughout the year between 1 April 1994 and 31 March 1995 as their “intensive observation period” (IOP). In this paper, we investigate the radar echo statistics using the IOP radar data set with synoptic charts twice a day (00 UTC and 12 UTC) provided by the German Meteorological Office.

### 3. Radar echo characteristics

#### 3.1. Radar echo appearance frequency with height

Seasonal variations of the precipitation were investigated using the appearance frequency of the radar echoes, which are shown in Fig. 2. Each panel shows the monthly appearance frequencies of the radar echoes with height, classified by season. The radar reflectivity was averaged over 30 min at first; cases of stronger reflectivity than 10 dBZ were counted. As the ground clutters from the side effect of the antenna contaminate the radar data, their corresponding heights are shaded in the panel. The seasonal variations of the radar appearance frequencies can be summarized as follows: In spring (Fig. 2a: April, May and March), most of the radar echoes appeared below 3 km AGL and the frequencies increased drastically as the height decreased. In summer (Fig. 2b: June, July, August and September), radar echo frequencies appeared above 4 km AGL, reaching as high as 6 km AGL in June and July. In fall (Fig. 2c: October, November and December), the frequencies increased below 1.8 km AGL. Compared with summer, the frequencies decreased above this level. In winter (Fig. 2d: January and February), most of the radar echoes appeared below 4 km AGL; appearance frequencies were small and almost independent of height.

The seasonal variations of the temperature profiles from April 1994 to March 1995 at Ny-Ålesund are shown in Fig. 3. Upper air soundings were taken by the Alfred Wegener Institute for Polar and Marine Research at Ny-Ålesund and the obtained temperature profiles were averaged over a month. In spring except March 1995, the monthly averaged temperatures were about  $-5^{\circ}\text{C}$  at the ground and decreased monotonically with height. The temperature profile in March was about  $5^{\circ}\text{C}$  lower than that in April and May. The radar echo appearance frequency was smaller in March than that in April and May. In summer, the monthly averaged ground air temperatures were between 0 and  $5^{\circ}\text{C}$ , warmest in July, followed by June and August and coldest in September. The temperature profiles were almost the same in June and August. The radar echo appearance frequencies most frequently appeared in July, followed by June and September and least in August. Compared to July, echoes in September appeared more frequently below 2.3 km AGL and less above this height. In autumn, the temperature profiles were almost the same in October, November and December. Ground air temperatures were around  $-10^{\circ}\text{C}$ . Most of the radar echoes appear below 1.8 km AGL in the autumn months (October to December). Temperature profiles in winter are almost the same as in January and February. Ground air temperatures are colder than  $-10^{\circ}\text{C}$ . Radar echo appearance frequencies are smallest in winter as are their height dependencies. Figure 4 shows the seasonal variations of the saturated

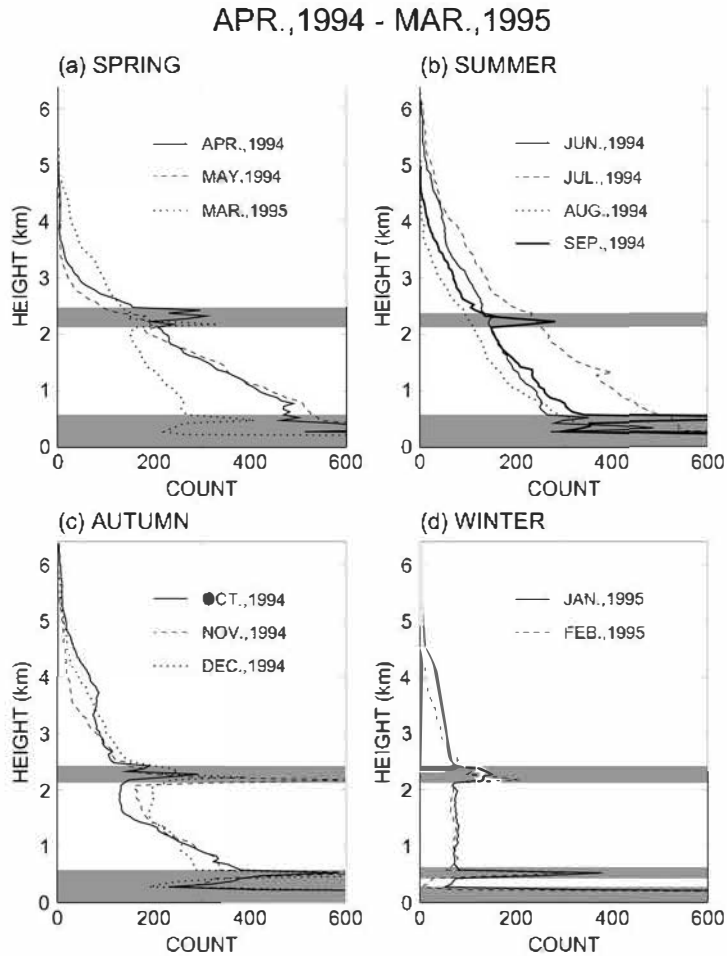


Fig. 2. Seasonal variations of radar echo appearance frequency profiles. (a) Spring; April (solid line), May (dashed line) and March (dotted line). (b) Summer; June (solid line), July (dashed line), August (dotted line) and September (thick solid line). (c) Autumn; October (solid line), November (dashed line) and December (dotted line). (d) Winter; January (solid line) and February (dashed line). Contaminations by ground clutter are shaded.

mixing ratio evaluated with the temperature profiles in Fig. 3. Compared with monthly appearance frequency profiles in Fig. 2 and monthly mean saturated mixing ratio profiles in Fig. 4, we can identify roughly consistency each other. As warmer air is able to contain a larger amount of water vapor, radar echo appearance frequencies are roughly proportional to the air temperature.

### 3.2. Typical radar echo patterns

Typical examples of the radar echoes in each season are shown in Fig. 5. Taking synoptic charts into account, four patterns of radar echoes can be found, labeled “A” to “D” in the panel. In Type A, the radar echoes have a pattern of deep echoes, which

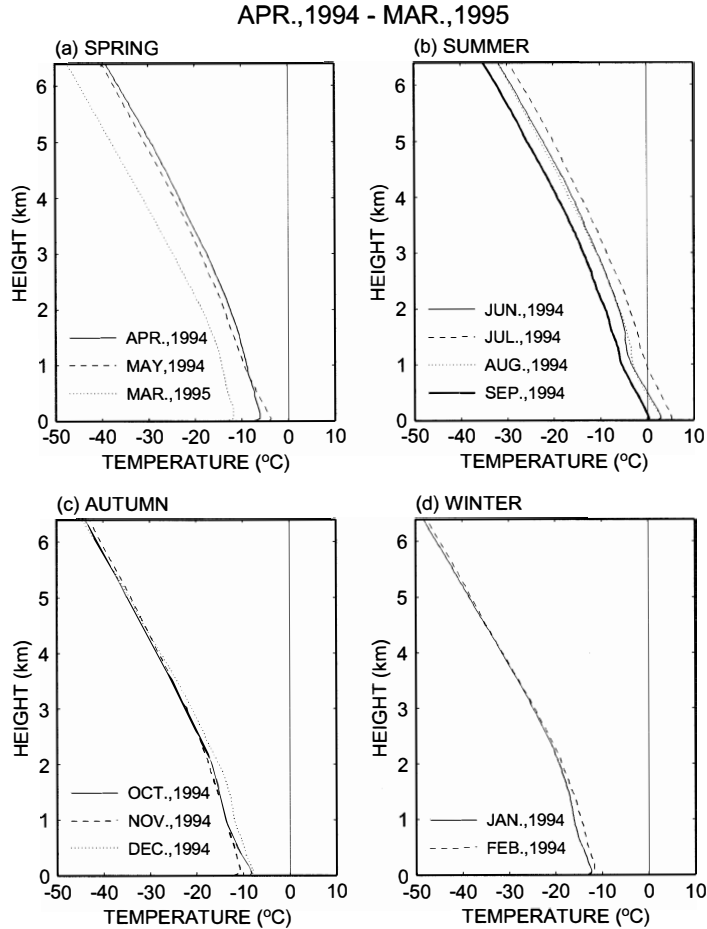


Fig. 3. Seasonal variations of air temperature profiles at Ny-Ålesund. Each profile is averaged over a month. The upper air sounding dataset is provided by the Alfred Wegener Institute for Polar and Marine Research. (a) Spring; April (solid line), May (dashed line) and March (dotted line). (b) Summer; June (solid line), July (dashed line), August (dotted line) and September (thick solid line). (c) Autumn; October (solid line), November (dashed line) and December (dotted line). (d) Winter; January (solid line) and February (dashed line).

touch on the ground, and have relatively long duration. In Type B, they also have long duration, but in this case echoes appear at the upper level and they do not touch on the ground. In Type C, the radar echoes are shallow, have uniform echo tops and have longer durations. In Type D, they have deep and strong reflectivity, touch on the ground, and have relatively short durations. The surface synoptic chart on each day marked ▼ in Fig. 5 is shown in Fig. 6. Synoptic charts show that echo patterns of Types A and B are associated with low pressure systems. The echo pattern of Type C corresponds to mixing boundary layer clouds over the open sea and Type D to deep convective clouds. These types are identified from the radar echo and synoptic chart.

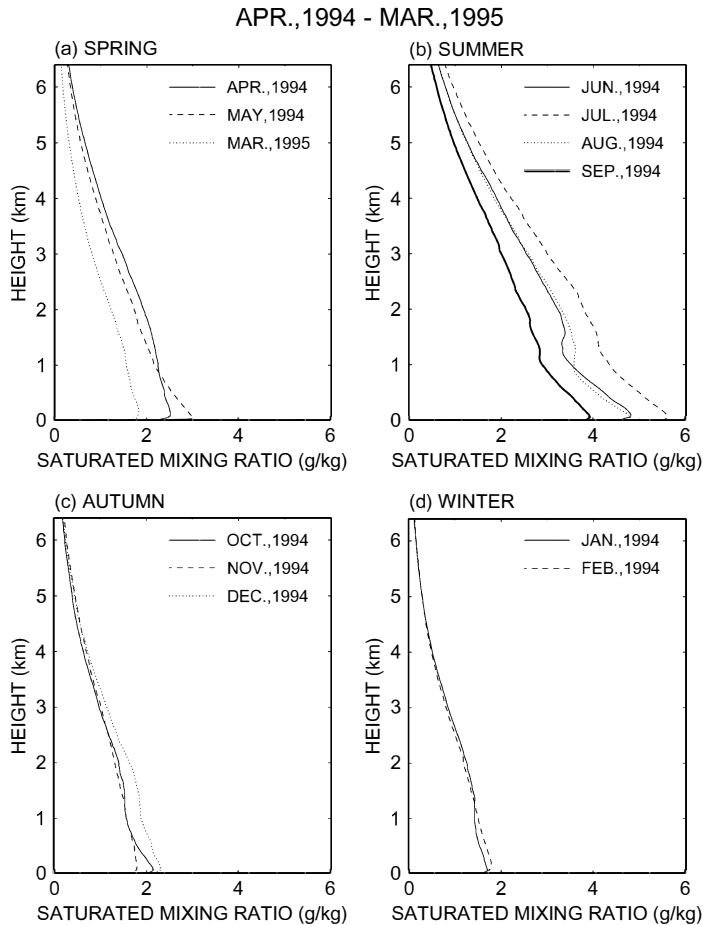


Fig. 4. Seasonal variations of saturated mixing ratio profiles evaluated based on Fig. 3. (a) Spring; April (solid line), May (dashed line) and March (dotted line). (b) Summer; June (solid line), July (dashed line), August (dotted line) and September (thick solid line). (c) Autumn; October (solid line), November (dashed line) and December (dotted line). (d) Winter; January (solid line) and February (dashed line).

Each type appearance frequencies in each month are shown in Fig. 7. Type A appears throughout the year, having peaks in summer (July) and early winter (December). Type B appears only in cold seasons (October–March) and has a maximum in February. Both Types A and B are related to low pressure system passage near the Svalbard archipelago. They accounted for over half of all radar echo appearances (Types A–D). Type C (boundary layer clouds) mostly occurs in spring (April–June) and early fall (August–December), while Type D (short-lived deep convective clouds) appears in summer (June–August). Characteristic mean and seasonal mean parameters of each type of radar echo are summarized in Table 1. Type A shows the largest of total number and duration among the 4 types. Although the longest duration

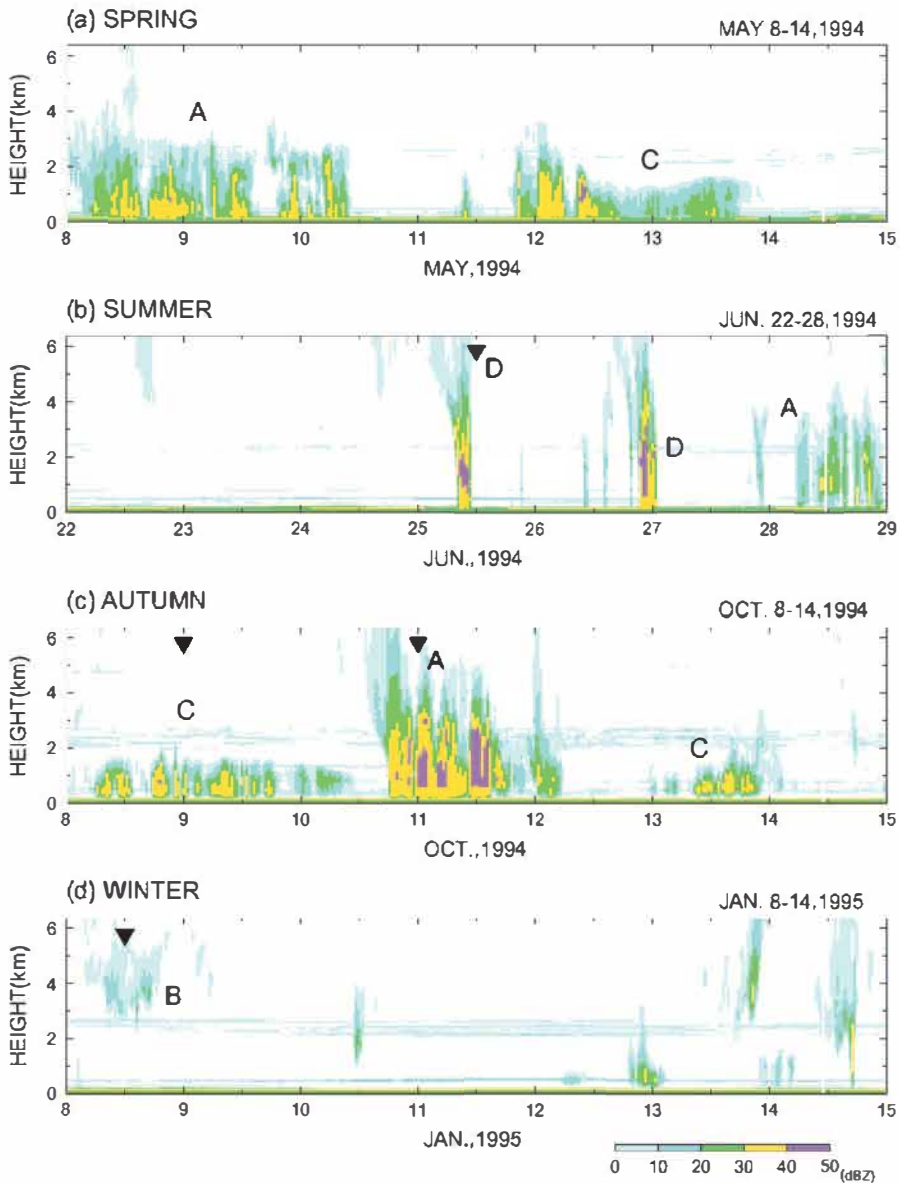


Fig. 5. Examples of the typical radar echo variation for each season. (a) Spring, May 8–14, 1994. (b) Summer, June 22–28, 1994. (c) Autumn, October 8–14. (d) Winter, January 8–14. Echo types are designated 'A' to 'D' in each panel. '▼' shows the surface weather map in Fig. 6. Horizontally extended echoes around 2–2.5 km AGL in each panel are ground clutter due to the side effect of the antenna.

appears in spring, larger depth, reflectivity, maximum height and total number appear in summer and autumn. Type B shows the largest maximum height and smallest reflectivity among the 4 types. Although the total number was largest in winter, the largest

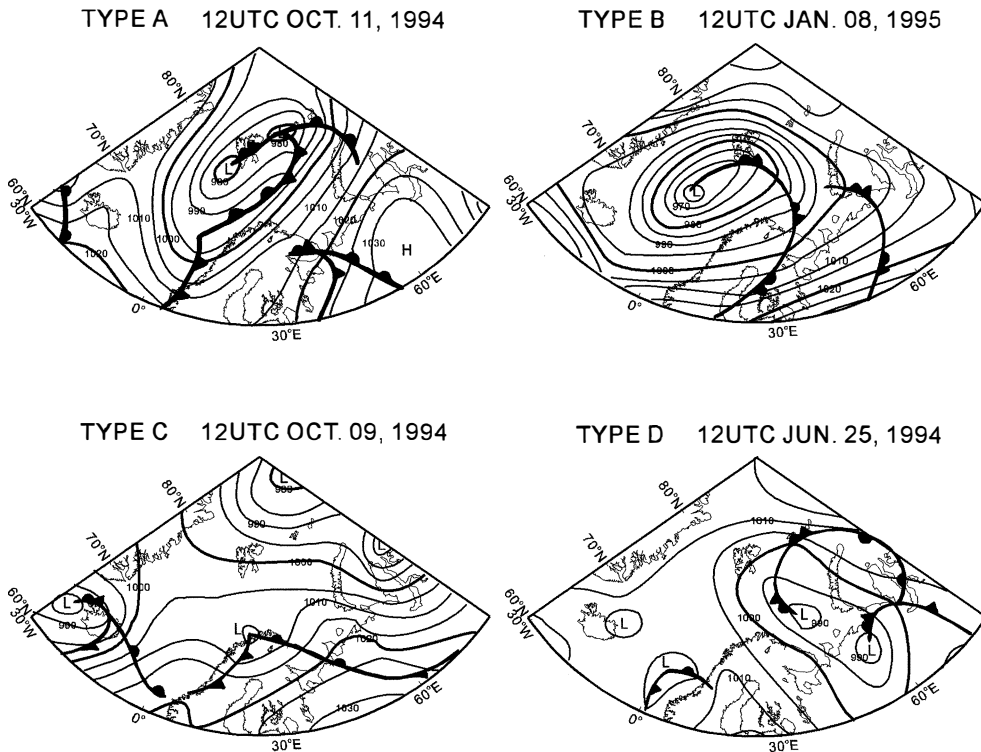


Fig. 6. Surface weather charts of each echo type 'A' to 'D.'

depth and reflectivity appeared in autumn. Type C shows the smallest depth and maximum height among the 4 types. Larger depth, reflectivity and duration appeared in spring and smaller depth, reflectivity and duration in summer. Type D shows the largest depth and reflectivity, and the smallest total number and duration.

#### 4. Low pressure systems around Svalbard

To understand low pressure system activity near the Svalbard archipelago, their frequency has been investigated in the surrounding region using weather charts issued by the German Meteorological Office between 1 April 1994 and 31 March 1995. The target area for the analysis is between 70°N and 85°N latitude and 20°W and 50°E longitude as shown in Figs. 1a and 8a. This area includes parts of the Norwegian Sea, Barents Sea and Arctic Ocean. A low pressure system is defined as being enclosed by a closed isobar on the surface weather chart. Results are shown in Fig. 8. A total of 71 low pressure systems were analyzed in this region for the year. On average, 5.9 low pressure systems were analyzed in this area in a month. The monthly frequencies are shown in Fig. 8b. The storm activities have wide seasonal variations. The occurrence frequency has maxima in fall and early winter (October, November and December), and a minimum in early summer (June). The second minimum appears in February.

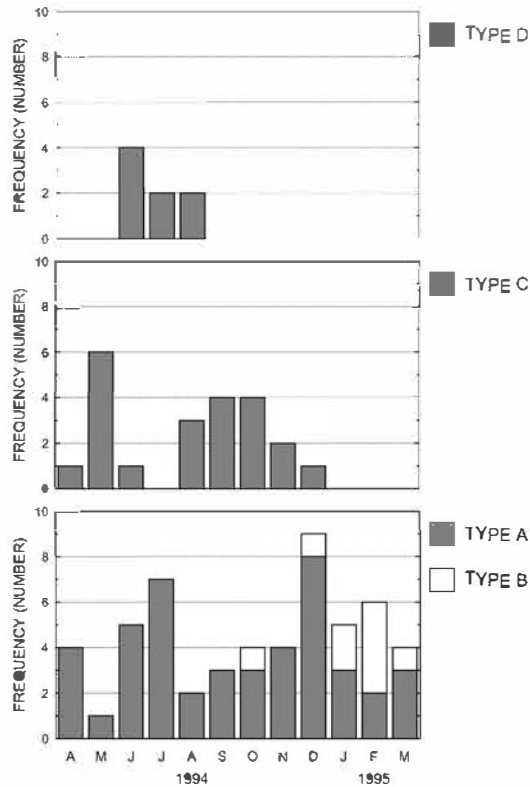


Fig. 7. Monthly frequencies of echo type appearance.

Among 71 low pressure systems (Fig. 8a), over 80% (57) move into the analyzed region, 45 (63%) traveling from the south over the Norwegian Sea, and the rest (14, 20%) originating in this region. It is found that low pressure systems are generated in this area only during spring and fall. The number of cyclones moving into this area increases in early winter (December and January).

The monthly mean minimum surface pressure of the lows and the monthly frequency of rapid intensified lows ( $>10$  hPa/24 h) are shown in Fig. 9. On average over a year, the minimum surface pressure is 980.7 hPa. Low pressure systems are weaker in spring and summer (April–September), and stronger in fall and winter. The minimum surface pressure is 990.0 hPa in September, and decreases to 964.4 hPa in December. Rapidly deepened low pressure systems also appeared over open water in the Norwegian Sea and Barents Sea in the cold seasons (fall and winter). Rapidly deepening low pressure systems (pressure fall exceeding 20 hPa over 24 hours) appear in October and January. The trajectories of low pressure systems in April, July, October and February are also shown in Fig. 10. Low pressure systems move zonally in the southern Norwegian Sea during mid-winter (February), in the northern Norwegian Sea during summer (July), and in the center during autumn (October) and early winter. They tend to meander during the warm seasons (spring and summer) and move directly

Table 1. Total and seasonal mean specific parameters of each echo type.

**TOTAL**

TYPE / SEASON	Average Depth (km)	Average Reflectivity (dBZ)	Maximum Depth (km)	Maximum Reflectivity (dBZ)	Maximum Height/Temp. (km/°C)	Total Number	Average Duration (hour)
TYPE A	1.9	21.4	3.7	34.9	4.2/-25.5	45	27.6
TYPE B	1.3	16.0	2.8	28.4	4.6/-28.1	9	19.6
TYPE C	0.9	20.3	1.4	35.6	1.6/-11.3	22	24.3
TYPE D	2.5	22.3	4.3	40.4	4.5/-27.5	8	3.6

**TYPE A**

TYPE / SEASON	Average Depth (km)	Average Reflectivity (dBZ)	Maximum Depth (km)	Maximum Reflectivity (dBZ)	Maximum Height/Temp. (km/°C)	Total Number	Average Duration (hour)
SPRING	1.9	21.5	3.5	42.4	3.9/-25.8	8	49.3
SUMMER	2.1	21.8	3.8	26.6	4.2/-17.5	17	25.7
AUTUMN	2.0	21.9	3.9	40.1	4.5/-31.4	15	23.3
WINTER	1.6	19.2	3.4	37.7	4.1/-32.2	5	16.7

**TYPE B**

TYPE / SEASON	Average Depth (km)	Average Reflectivity (dBZ)	Maximum Depth (km)	Maximum Reflectivity (dBZ)	Maximum Height/Temp. (km/°C)	Total Number	Average Duration (hour)
SPRING	1.2	15.2	2.4	26.6	5.3/-34.8	1	11.5
SUMMER	-	-	-	-	-	-	-
AUTUMN	1.4	16.9	3.1	34.9	4.9/-33.8	2	28.8
WINTER	1.3	15.8	2.7	25.5	4.3/-33.3	6	17.1

**TYPE C**

TYPE / SEASON	Average Depth (km)	Average Reflectivity (dBZ)	Maximum Depth (km)	Maximum Reflectivity (dBZ)	Maximum Height/Temp. (km/°C)	Total Number	Average Duration (hour)
SPRING	1.1	21.2	1.7	38.0	1.2/-11.6	7	31.1
SUMMER	0.7	18.5	1.0	32.3	1.2/-3.8	8	17.1
AUTUMN	0.9	21.5	1.4	36.9	1.7/-15.1	7	25.4
WINTER	-	-	-	-	-	-	-

**TYPE D**

TYPE / SEASON	Average Depth (km)	Average Reflectivity (dBZ)	Maximum Depth (km)	Maximum Reflectivity (dBZ)	Maximum Height/Temp. (km/°C)	Total Number	Average Duration (hour)
SPRING	-	-	-	-	-	-	-
SUMMER	2.5	22.3	4.3	40.4	4.5/-19.4	8	3.6
AUTUMN	-	-	-	-	-	-	-
WINTER	-	-	-	-	-	-	-

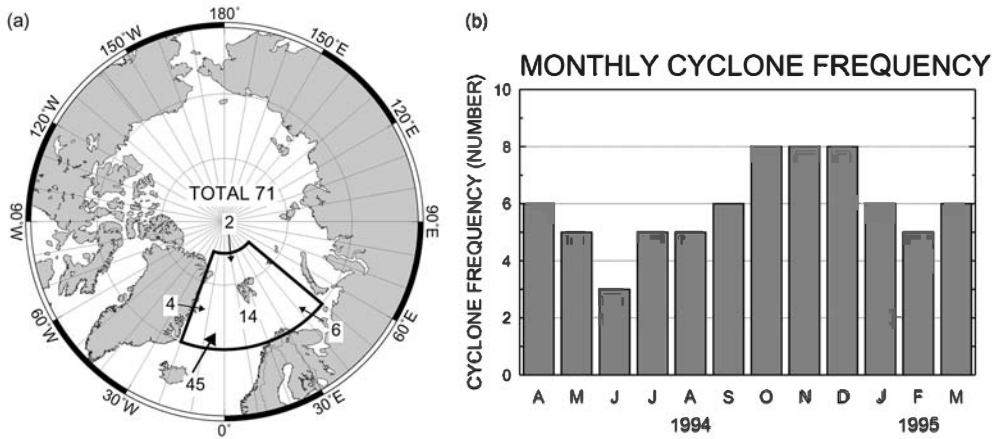


Fig. 8. Occurrence frequencies and movement of low pressure systems. (a) Occurrence frequencies and direction of movement into the analysis area. (b) Monthly occurrence frequencies.

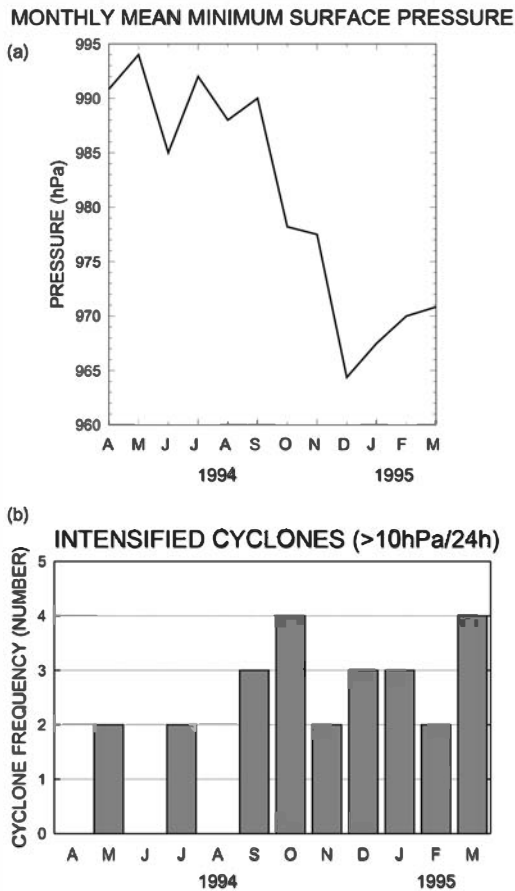


Fig. 9. Monthly variations of the averaged minimum surface pressure of the low pressure system (a) and monthly frequency of intensified cyclones (b). An intensified cyclone is defined as a cyclone with rapidly deepening minimum surface pressure, exceeding 10 hPa in 24 hours.

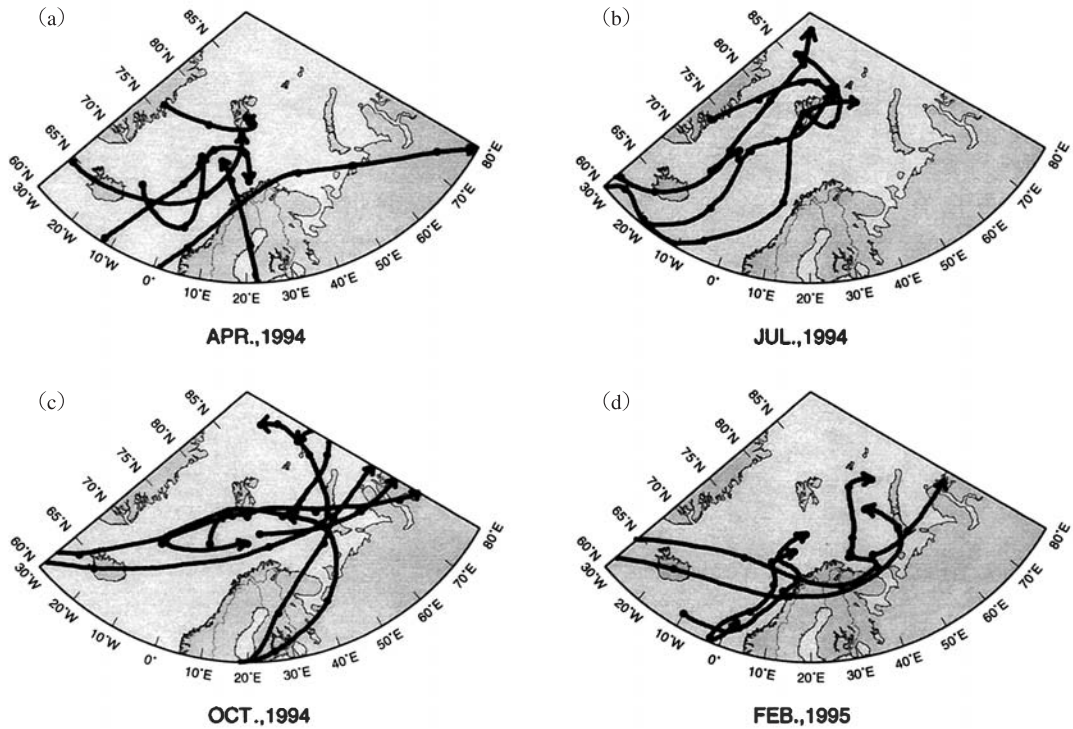


Fig. 10. Cyclone trajectories. (a) April, 1994, (b) July, 1994, (c) October, 1994 and (d) February, 1995.

during cold seasons (autumn and winter). They are also weaker during warm seasons and intensified in the cold seasons (autumn and early winter).

Climatological research works with radar echoes in a high Arctic region such as Ny-Ålesund ( $78^{\circ}55'N$ ) seldom appear in the literature. Generally, precipitable water in the high Arctic is very little due to the cold air temperature. Low pressure systems contribute to transport of warm air and moisture into the high Arctic from lower latitude. The monthly averaged vertically integrated poleward vapor fluxes have been investigated over the Norwegian Sea between  $20^{\circ}W$  and  $30^{\circ}E$  in longitude over the  $70^{\circ}N$  latitude between April 1994 and March 1995. The result shows two prominent peaks in July and December (not shown here). The monthly variations are similar to the monthly echo pattern related to low pressure systems (TYPES A + B).

## 5. Summary

This is a preliminary report on radar echo characteristics at Ny-Ålesund, Svalbard, Norway. Using X-band vertically pointing radar data at Ny-Ålesund and synoptic weather charts, characteristics of radar echoes are examined for one year between April 1994 and March 1995. Each series of radar echoes is classified into four patterns taking account of synoptic conditions, and strong seasonal variations are found. Low pressure system patterns appear throughout the year, occupying over half of all radar echo

appearances, and have peaks in early summer and early winter. Low pressure systems over the Norwegian Sea also have strong seasonal variations. The occurrence frequency has a maximum in fall and early winter and a minimum in early summer. They move zonally over the southern Norwegian Sea during mid-winter, over the northern Norwegian Sea during summer, and over the center during autumn and early winter. These storm activities are consistent with the radar echo behavior at Ny-Ålesund.

The period which is analyzed in this paper, is only one year, from April 1994 to March 1995, and seasonal variations are emphasized in this paper. However, inter-annual variations are one of the most important topics in climatology and global warming. To understand further Arctic weather and climate systems, additional long-term observations including weather radar observations and storm research are necessary around the Svalbard archipelago and in fact the entire Arctic region.

### Acknowledgments

The authors would like to express their thanks to Naohiko Hirasawa and two anonymous reviewers for encouragement and constructive comments. This research was partially supported by a “Grant-in-Aid for Science Research” of the Ministry of Education, Culture, Sports, Science and Technology of Japan (Monbu-kagaku-sho).

### References

- Cullather, R.I., Bromwich, D.H. and Serreze, M.C. (2000): The atmospheric hydrologic cycle over the Arctic Basin from reanalyses. Part I: Comparison with observations and previous studies. *J. Climate*, **13**, 923–937.
- Newell, R.E. and Zhu, Y. (1994): Tropospheric rivers: A one-year record and a possible application to ice core data. *Geophys. Res. Lett.*, **21**, 113–116, 10.1029/93GL03113.
- Oshima, K. and Yamazaki, K. (2004): Seasonal variation of moisture transport in polar regions and the relation with annular modes. *Polar Meteorol. Glaciol.*, **18**, 30–53.
- Serreze, M.C. and Barry, R.G. (1988): Synoptic activity in the Arctic Basin, 1979–85. *J. Climate*, **1**, 1276–1295.
- Serreze, M.C. and Barry, R.G. (1995): Atmospheric water vapor characteristics at 70°N. *J. Climate*, **8**, 719–731.
- Serreze, M.C., Box, J.E., Barry, R.G. and Walsh, J.E. (1993): Characteristics of Arctic synoptic activity, 1952–1989. *Meteorol. Atmos. Phys.*, **51**, 147–164.
- Wada, M., Konishi, H. and Yamanouchi, T. (1997): Variation of monthly precipitation and frequency of radar echo existence at some altitudes in Ny-Ålesund, Svalbard, Arctic. *Mem. Natl Inst. Polar Res., Spec. Issue*, **51**, 239–246.